

Extended SIRU model with dynamic transmission rate and its application in the forecasting of COVID-19 under temporally varying public intervention

Yiye Jiang^{1,*}, Gaston Vergara-Hermosilla²

¹Université Grenoble Alpes, CNRS, Inria,
Grenoble INP, LJK, Grenoble, France
yiye.jiang@inria.fr  0000-0001-8464-4038

²Institut de Mathématiques de Bordeaux,
Université de Bordeaux, Talence, France
gaston.v-h@outlook.com  0000-0002-3055-8406

Dedicated to the memory of professor Pierre Magal.

Received: October 14, 2023, Accepted: December 17, 2024, Published: December 31, 2024

Abstract: By considering the recently introduced SIRU model, in this paper we study the dynamic of COVID-19 pandemic under the temporally varying public intervention in the Chilean context. More precisely, we propose a method to forecast cumulative daily reported cases $CR(t)$, and a systematic way to identify the unreported daily cases given $CR(t)$ data. We firstly base on the recently introduced epidemic model SIRU (Susceptible, Asymptomatic Infected, Reported infected, Unreported infected), and focus on the transmission rate parameter τ . To understand the dynamic of the data, we extend the scalar τ to an unknown function $\tau(t)$ in the SIRU system, which is then inferred directly from the historical $CR(t)$ data, based on nonparametric estimation. The estimation of $\tau(t)$ leads to the estimation of other unobserved functions in the system, including the daily unreported cases. Furthermore, the estimation of $\tau(t)$ allows us to build links between the pandemic evolution and the public intervention, which is modeled by logistic regression. We then employ polynomial approximation to construct a predicted curve which evolves with the latest trend of $CR(t)$. In addition, we regularize the evolution of the forecast in such a way that it corresponds to the future intervention plan based on the previously

obtained link knowledge. We test the proposed predictor on different time windows. The promising results show the effectiveness of the proposed methods.

Keywords: SIRU model, transmission rate, cumulative daily reported cases, nonparametric estimation

I. INTRODUCTION

In the recent years, the modelling of epidemiological phenomena has played a protagonist role in taking decisions and controlling the COVID-19 pandemic around the world [1]. In particular, mathematical approaches have made significant contributions, for their abilities to help understand and predict the underlying patterns of the epidemiological dynamics [2]. We refer to the review paper [3], which provides a comprehensive overview of recently proposed mathematical models for COVID-19 studies. The paper shows that one popular way of modelling is by employing the compartmental models, which are the classical models initially designed for general infectious diseases. For

Copyright: © 2024 Yiye Jiang, Gaston Vergara-Hermosilla. This article is distributed under the terms of the Creative Commons Attribution License (CC BY 4.0), which permits unrestricted use, distribution, and reproduction in any medium, provided the original author and source are credited.

*This author conducted this work while she was preparing her PhD at Université de Bordeaux. Corresponding author

Citation: Yiye Jiang, Gaston Vergara-Hermosilla, Extended SIRU model with dynamic transmission rate and its application in the forecasting of COVID-19 under temporally varying public intervention, Biomath 13 (2024), 2412176, <https://doi.org/10.55630/j.biomath.2024.12.176>

example, the authors of [4, 5] based their studies on the SEIR (Susceptible, Exposed, Infected, Removed) model, while the authors of [6, 7] relied on the SIRD (Susceptible, Infected, Recovered, Dead) model.

On the other hand, researchers of the machine learning community have also used their expertise in the modelling of the COVID-19. For instance, the authors in [8] applied tools from functional data analysis to model the trajectories of cumulative daily reported cases across countries, while the authors of [9] adopted the point-process-based approaches to model the infection/death cases which can be considered as events arriving at random times. Some other papers considering machine learning methods that we highlight here are [10–12]. However, the approaches from the two research communities were proposed relatively independently. Thus, in this paper, we consider machine learning techniques with a compartmental model to perform an efficient modelling of COVID-19.

We focus on the recently introduced compartmental model SIRU [2]. SIRU model [2] has been successfully implemented to describe the evolution of COVID-19 during the first pandemic waves in several countries, such as China, South Korea, Italy and France. More importantly, it introduces the compartment *unreported cases* to the modelling, which consider the dynamical role of unidentified infected cases in the evolution of the epidemic. At this point, we stress the fact that, from the beginning of the pandemic, related research works have been proposed to deal with the unreported cases and their role in the progression of the epidemic, where we highlight the papers [13] and [14]. The existence of unreported cases is caused by, first, the cases who never manifest symptoms during the infection, and secondly, the low testing capacity in certain countries or regions. Regardless its wide existence, it can not be observed. Thus inferring this quantity is of great interest.

Our work is motivated by noticing that the initial SIRU model as well as its later variants all use relative simple representations of the transmission rate, which are not consistent with the reality, especially when public intervention changes along time. Thus we start from this point, and aim to equip the SIRU model with a way to construct a time varying transmission rate, which is moreover derived from real data. In the following we firstly recall the initial SIRU model.

SIRU model describes the dynamic of an epidemic by a system of ordinary differential equations (ODEs), which involves four unknown functions representing four compartments: susceptible individuals, asymptomatic infected individuals who do not yet have symp-

toms, symptomatic reported infected individuals, and symptomatic unreported infected individuals, denoted by S , I , R and U , respectively. The proposed dynamic is illustrated by the diagram flux in Figure 1 (see also [2]).

The corresponding system of ODEs reads as:

$$\begin{cases} S'(t) = -\tau S(t)(I(t) + U(t)), \\ I'(t) = \tau S(t)(I(t) + U(t)) - \nu I(t), \\ R'(t) = \nu_1 I(t) - \eta R(t), \\ U'(t) = \nu_2 I(t) - \eta U(t), \end{cases} \quad (1)$$

where $\nu = \nu_1 + \nu_2$, and $\tau, \nu, \nu_1, \nu_2, \eta$ are all positive. As usual, the system is supplemented with initial data:

$$\begin{aligned} S(t_0) &= S_0 > 0, & I(t_0) &= I_0 > 0, \\ R(t_0) &= 0 & \text{and } U(t_0) &= U_0 \geq 0. \end{aligned} \quad (2)$$

The meanings of all involved parameters in Model (1) are summarized in Table 1.

We remark that, in the initial works on the SIRU model [2, 15], the initial data are derived by assuming the early stage of the system is exponential, and the parameters ν, f, η are treated as hyperparameters, which means that they are pre-assigned but not learnt from real data. We use the same practice in our work. Thus, the transmission rate τ will be the key parameter to control the epidemic propagation after the early stage. This implies that, a better τ will make the SIRU system closer to real situations in the sense that the $CR(t)$ recovered from the SIRU solution is closer to the real observation. In this case, the other SIRU solutions $S(t), R(t), U(t)$ will be more reliable estimations of the unobserved data.

To furthermore adapt the SIRU model to the situation where the transmission rate is influenced by the public interventions, the authors of [15] and [16], proposed to make the transmission rate τ as a function of time, parametrized by the public intervention. More precisely, in [16], the authors propose the following structure of the transmission rate:

$$\tau(t) = \begin{cases} \tau_0, & \text{for } t \in [t_0, t_1], \\ 0, & \text{for } t \geq t_1, \end{cases} \quad (3)$$

while in [15] the authors consider:

$$\tau(t) = \begin{cases} \tau_0, & \text{for } t \in [t_0, t_1], \\ \tau_0 \exp(-\mu(t - t_1)), & \text{for } t \geq t_1, \end{cases} \quad (4)$$

where τ_0 is a scalar parameter which characterises the constant transmission rate during the time interval $[t_0, t_1]$, and μ is a scalar parameter that characterises the constant intervention intensity. In both cases, even

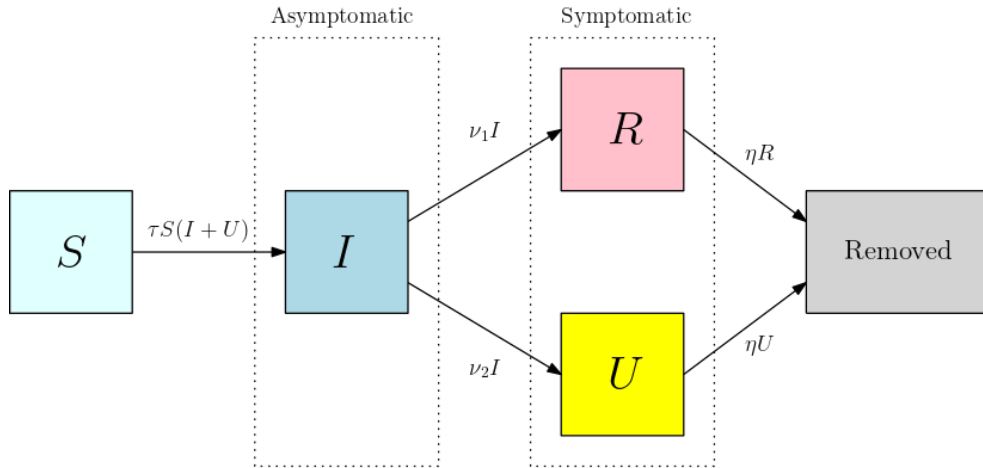


Fig. 1: Diagram flux associated with the SIRU model.

Parameters	Interpretation
t_0	Time at which the epidemic started.
S_0	Number of individuals susceptible to the disease at time t_0 .
I_0	Number of infected individuals without symptoms at time t_0 .
R_0	Number of reported infected individuals at time t_0 .
U_0	Number of unreported infected individuals at time t_0 .
τ	Transmission rate of the disease.
$1/\nu$	Average time during which the infected asymptomatic individuals remain asymptomatic.
f	Fraction of asymptomatic infected individuals that become reported infected individuals.
$\nu_1 = f\nu$	Rate at which asymptomatic infected cases become reported symptomatic.
$\nu_2 = (1 - f)\nu$	Rate at which asymptomatic infected cases become unreported infected.
$1/\eta$	Average time during which an infected individual presents symptoms.

Table 1: Parameters of the SIRU model.

with these more detailed model designs for $\tau(t)$, the numerical results still end with one pandemic wave, as the initial SIRU construction. However, the data obtained from the official statistics of all countries show multiple waves. Thus, it is important to find a more powerful and flexible model construction for the transmission rate.

On the other hand, in [17], the authors proposed a more sophisticated form of the transmission rate which considers r intervention intensity values as in Equation (5).

$$\tau(t) = \begin{cases} \tau_0, & \text{for } t \in [t_0, t_1], \\ \tau_1(t) = \tau_0 \exp(-\mu_1(t - t_1)), & \text{for } t \in [t_1, t_2], \\ \vdots \\ \tau_r(t) = \tau_{r-1}(t_r) \exp(-\mu_r(t - t_r)), & \text{for } t \in [t_r, t_{r+1}]. \end{cases} \quad (5)$$

Even though the large number of parameters is potentially able to capture the complicated dynamic of transmission rate, finding the ideal parameter values which can correctly reconstruct the real data became another problem. In fact, the values of $t_i, i = 0, \dots, r + 1$ need to be either manually tuned or extensively searched over grids, both by comparing with the data. Thus we were to search for a method which can not only bring high variability to τ but also is easy to estimate. Considering the tuning difficulty is inevitable for any parametric forms imposed to $\tau(t)$, for data illustrating multiple waves, we propose to make τ a fully free function of time and to use the nonparametric estimation in the SIRU system to infer the shape of the function directly from the real data. This initiative makes the classical compartmental model fully benefit the data so as to give a precise reconstruction of transmission rate dynamic. The resulting estimation method of the transmission rate is the primary result of this paper. We then link transmission rate to the changes of public intervention

in order to study the influence of the latter. The result will serve for the forecasting of the cumulative number of symptomatic reported infected cases $CR(t)$, which can thus take into account the future intervention plans. Such forecasting models are of great interest for the decision makers. In the following, we resume the main novelties of the proposed methods, and present the organization of this article.

Contributions of the paper: The main contributions of this article are twofold:

- 1) firstly, a nonparametric method is proposed to estimate the transmission rate $\tau(t)$ which is consistent with both the SIRU system and the real data;
- 2) secondly, a new method is proposed to predict the cumulative number of reported symptomatic infected cases $CR(t)$ which takes into account the varying public intervention and a long prediction period.

Organization of the paper: In Section II-A, we propose the nonparametric method to estimate the transmission rate $\tau(t)$ as well as the estimations of $I(t), R(t), S(t)$ and the unreported daily cases $U(t)$. In Section II-B, we rely on the logistic regression to predict from the temporal variable public intervention $Q(t)$ the dynamic of $\tau(t)$. In Section II-C, we consider the prediction of $CR(t)$. We propose the regularized polynomial approximation as the predictor. It is defined as a minimizer of an optimization problem which considers simultaneously the historical data of $CR(t)$, and the predicted future $\tau(t)$ dynamic. Finally, in Section III, we present the numerical evidence of the proposed methods.

II. METHODOLOGY

A. Nonparametric estimation of the transmission rate

In this section, we propose a method to infer the curve of transmission rate $\tau(t)$. We require the inferred values to be reliable, in the sense that they are able to recover the observed cumulative number of reported infected cases $CR(t)$ with good accuracy, when plugged back into the SIRU model. Given the observations of $CR(t)$ at time instants t_1, \dots, t_N , we propose to make $\tau(t)$ an unknown function to be solved, instead of providing an explicit form as in literature. In return, we make $I(t)$ a known function in SIRU (1) system by estimating it outside the system using its dependency with the observation $CR(t)$:

$$CR(t) = \nu_1 \int_{t_0}^t I(s) ds. \tag{6}$$

The resolution of this transformed SIRU model gives the inferred transmission rate function, together with the reliable reconstructions of $S(t), R(t)$ and $U(t)$.

To get a function, which is highly close to the “true” $I(t)$ under the SIRU model assumption, we first apply an admissible nonlinear approximation on the $CR(t)$ data to obtain the estimated curve $\widehat{CR}(t)$. Then the relationship between $I(t)$ and $CR(t)$ in Equation (6) implies that the estimators for $I(t)$ and $I'(t)$ can be defined as

$$\widehat{I}(t) = \widehat{CR}'(t) / \nu_1. \tag{7}$$

Therefore, we can plug the estimated functions $\widehat{I}, \widehat{I}'$ in the SIRU model, and consider the resulting ODE system as the system of $S(t), R(t), U(t), \tau(t)$, which reads as

$$\begin{cases} S'(t) = -\tau(t)S(t)(\widehat{I} + U(t)), \\ R'(t) = \nu_1 \widehat{I} - \eta R(t), \\ U'(t) = \nu_2 \widehat{I} - \eta U(t), \\ \widehat{I}'(t) = \tau(t)(\widehat{I} + U(t))S(t) - \nu \widehat{I}. \end{cases} \tag{8}$$

This system is equivalent to:

$$\begin{cases} S'(t) = -\widehat{I}' - \nu \widehat{I}, \\ R'(t) = \nu_1 \widehat{I} - \eta R(t), \\ U'(t) = \nu_2 \widehat{I} - \eta U(t), \\ \tau(t) = \frac{\widehat{I}' + \nu \widehat{I}}{(\widehat{I} + U(t))S(t)}. \end{cases} \tag{9}$$

System (9) is easy to solve given the initial data S_0, R_0, U_0 and t_0 . The initial data is obtained in the same¹ manner as [2].

The key point in the above estimation is to choose an admissible nonlinear method. Common nonlinear methods that reconstruct a data curve by a function, are polynomial approximation, spline, and kernel smoother, see for example [18]. For Model (9), we propose to use the kernel smoother. On one hand, the polynomial approximation usually introduces oscillations, which will furthermore be amplified after taking derivatives. Thus the final estimated $\tau(t)$ will exhibit more local extreme points which will mislead the interpretation

¹It is worth mentioning that, to be consistent with the initial values, before applying the nonlinear approximation, we amend to the observations the data points $CR(t_0), \dots, CR(0)$ that are generated by the exponential estimation of early stage of $CR(t)$. The exponential estimation is the one used in the calculation of initial values.

of true dynamic contained in raw data. On the other hand, the $I'(t)$ expression given by the SIRU model (1) implies that $I(t)$ is likely to be a C^∞ function. Thus compared to spline function which is piece-wise polynomials of low order, the kernel smoother with Gaussian kernel is preferable.

To close this subsection, we comment that the non-parametric estimation we proposed to τ is transferable. That means, we can apply the same method over other hyperparameters as f, v, η . However, since only $I(t)$ is turned known, in return, to maintain exactly 4 unknowns for 4 equations, each time we can only make one of τ, f, v, η unknown (time-varying) with the rest presumed values which are fixed all the time. At this point, we privilege a functional τ . Because it is by nature more variable than other hyperparameters like average infected time, since the others are related to psychological facts. Thus it is less reasonable to let vary the others but set the transmission rate fixed all the way. On the other hand, transmission rate is the key characteristic of the evolution of epidemic, thus it is important to investigate it deeply. In the next subsection, we will use the transmission rate function in the further studies on the impact of changing government measures.

B. Logistic regression with the public intervention policies

In this section, we consider the case of variable public intervention measure. We wish to study its impact on the evolution of epidemic and develop the analysis, given the transmission rate data, and additionally the historical intervention data. To this end, we first introduce a new temporal function which is able to represent the intervention measure. Then we propose a mathematical model which describes the relationship between the introduced measure function and the transmission rate. The resulting model is expected to furthermore help the prediction of unseen $CR(t)$.

We illustrate our approach in Chile’s context. In Chile, a significant varying public measure is the percentage of national population in quarantine. Such measurement is used in the work of [17] to motivate the design the epidemic model, and leads to a good fit of $CR(t)$. We therefore consider the same measurement as the representative of overall public intervention. In Figure 2, we show the evolution of national quarantine percentage. The data is obtained from official information about quarantines provided by the ministry of health of the Chilean government via the webpage [25].

We especially smooth the data points to facilitate the observation. We can see that generally, the dynamic of the measurement is complicated. There exists several accelerations and decelerations of the implementation of quarantine. On the top of Figure 2 is the inferred transmission rate $\tau(t)^2$ obtained from the preceding section.

We can observe that, from the aspect of the two curve shapes, the extreme points of the transmission rate and the inflection points of the quarantine percentage coincide approximately in time, for example around 5/10/2020 and 6/29/2020. In order to furthermore study this potential link of dynamics, we denote the quarantine percentage at time instant t by $Q(t)$, whose values are located in $[0, 100]$. We require $Q(t) \in C^2(\mathbb{R})$. We also need to assume $\tau(t) \in C^1(\mathbb{R})$, notice that the inferred $\tau(t)$ by the proposed method belongs to $C^\infty(\mathbb{R})$. Thus, the observation indicates that, when the absolute value of $\dot{Q}(t)$ is small, it is very likely that the absolute value of $\dot{\tau}$ becomes small as well.

Recall that we aim to construct a model in terms of $\tau(t)$ and $Q(t)$, so that the fitted model can be used to predict the future behaviors of τ given the public intervention plans. Thus, we propose to adopt the logistic regression (see for example [18]), to predict the probability of the occurrence of event $\dot{\tau}(t) = 0$ at every time instant t . The proposed model is:

$$\begin{aligned}
 &P\left(\dot{\tau}(t) = 0 \mid \ddot{Q}(t), \dot{Q}(t)\right) \\
 &= \text{Sig}\left(\beta^\top \left[\mathbf{1}, \ddot{Q}(t), \left(\ddot{Q}(t)\right)^2, \dot{Q}(t), \left(\dot{Q}(t)\right)^2 \right]\right),
 \end{aligned}
 \tag{10}$$

where $\text{Sig}(\cdot)$ is the Sigmoid function. In practice, we smooth the data points to obtain the approximating function of $Q(t)$ (the red curve in Figure 2), so that we can calculate the derivatives. The details on this smoothing and the further training strategies³

²In the literature there is no mention nor discussion about the unit of transmission rate. Thus, here we give a reasonable interpretation, that is, transmission rate represents the probability of an individual from I (asymptomatic infected) or U (unreported symptomatic infected) infecting an individual from S (susceptible to be infected). The support of this interpretation is the equation of the SIRU model $S'(t) = -\tau S(t)(I(t) + U(t))$, which describes how much S individuals should become I individuals. Thus given the population, the value of transmission rate needs to be very small. Furthermore, we made the transmission rate time-varying, thus we can furthermore interpret the transmission rate at time t as the probability at time t of an individual from I or U infecting an individual from S .

³The event of this logistic regression model is $\dot{\tau} = 0$, which is a local extreme point of the transmission rate. However, there are only a few such points, for example, approximately 6 – 7 local extreme points in Figure 2 (left panel). Thus, we propose the particular strategies to compose large enough and balanced training set.

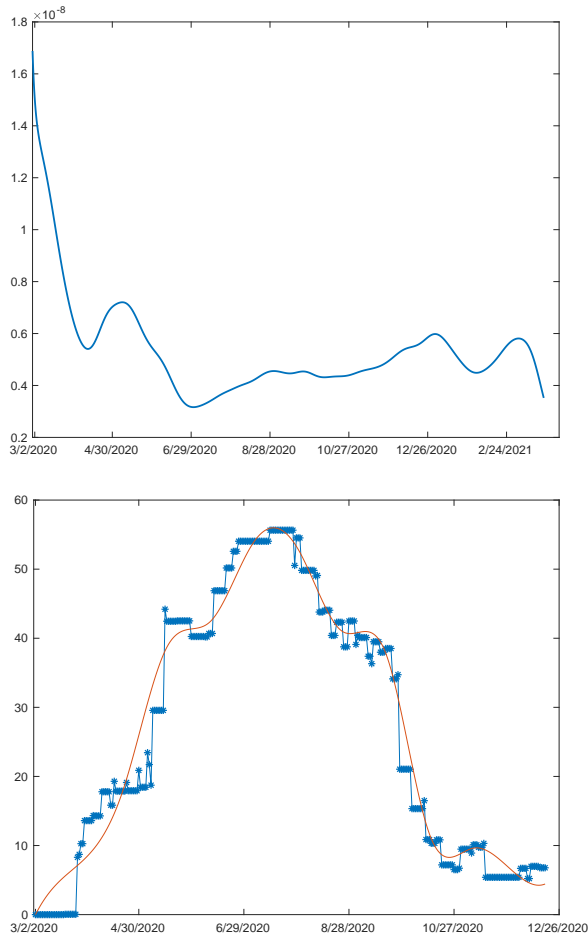


Fig. 2: Inferred transmission rate (left) from the Chilean COVID-19 data, percentages of the Chilean population in quarantine (right). The red curve in the right plot shows the smoothing curve of the discrete data points.

of Model (10) are given in the appendix. Therefore, the time instants \hat{t}_E with high predicted probabilities $P(\hat{\tau}(\hat{t}_E) = 0 \mid \hat{Q}(\hat{t}_E), \hat{Q}'(\hat{t}_E))$ (for example bigger than 0.9) can be considered as the predicted moments for the transmission rate to reach local extreme values.

Model (10) assumes that the likelihood of $\tau(t)$ to reach its local extreme values at time t depends on whether the government is changing the public intervention policies at that moment. To distinguish the impacts of changes between different public intervention policies, for example:

- from decelerating (accelerating) to accelerating (decelerating) the reinforcement of intervention,
- from accelerating (decelerating) to decelerating (accelerating) the relaxation of intervention,

we consider $\ddot{Q}(t)$, $\dot{Q}(t)$, and $(\dot{Q}(t))^2$ as dependent variables as well in the model. Note that we intentionally avoid quantitative models of $\tau(t)$, such as ordinary differential equation of $\tau(t)$, or regression model. Indeed, we have tested these ways of modelling.⁴ However, the testing results imply that the quantitative dependency of τ and Q can be very complicated. This brings to inevitable prediction errors. These errors will moreover be amplified in the retrieved $CR(t)$, when passing the predicted τ through the SIRU model.

C. Prediction of $CR(t)$

Recently, many works have considered the forecasting of cumulative reported infected cases, for example [10, 19–21]. However, some of them propose the methods only valid for the prediction over the first wave. At this point, we especially refer to the works in [20, 22, 23] which adopt the exponential smoothing models [24, Chapter 7]. The principle of such prediction models is to extrapolate the $CR(t)$ trend thus to obtain its forecasting. An big advantage of exponential smoothing methods is that they can be used indifferently for the forecasting of any time interval. Nevertheless, since the $CR(t)$ is extrapolated with curves of simple forms and little parametrization: exponential in [23] for EST(M,M,N) model, linear in [22] for EST(A,A,N) model, the length of satisfactory prediction interval is very limited. Starting from this point, we propose to use nonlinear function with adequate number of parameters to first fit the trend, and then extrapolate it with an additional control. We consider polynomials, because its analytic facility enables us to relate the predicted behavior of τ to the prediction of $CR(t)$ through SIRU model. To avoid Runge’s phenomenon associated to the polynomial approximation, especially the oscillation at the end of fitting interval, we sample the Chebyshev nodes in practice to fit the polynomial. The use of Chebyshev nodes can reduce the oscillation. Moreover, we consider the shape control of the polynomial, especially in the trend extrapolation part. We propose to fit the polynomial under the constraint given by the predicted $\tau(t)$ dynamic. Namely, we require the optimal polynomial to have the consistent characteristics so that its deduced transmission rate reaches the local extreme values around the previously predicted moments. Meanwhile we would like the optimal polynomial to be as similar as possible as $CR(t)$ in the fitting interval. The performance of the resulting predictor polynomial

⁴We fit the models with 80% of the historical data, and evaluate the prediction performance with the rest 20%.

has been significantly improved, where it recovers the $CR(t)$ values precisely for an ongoing month, as shown in Section III. We formalize the proposed forecasting method in the following optimization problem.

$$CR^* = \arg \min_{P(\cdot; \Theta) \in P_m} \frac{1}{N} \sum_{i=1}^N \left(CR(t_i) - P(t_i; \Theta) \right)^2, \tag{11}$$

subject to: $(\tau'_p(\hat{t}_E; \Theta))^2 \leq \lambda_0$.

In the above problem, P_m is the family of polynomials of order m , $CR(t_i)$, $i = 1, \dots, N$ are the data points of fitting interval, λ_0 is a pre-given positive hyperparameter, $\tau_p(t; \Theta)$ is the deduced transmission rate defined by the SIRU model (9) where $\widehat{CR}(t)$ is given as $P(t; \Theta)$, \hat{t}_E is the predicted moment when the transmission rate reaches the first local extreme value after time instant t_N . The constraint on the one hand addresses the oscillation problem of polynomial approximation, on the other hand, transfers the future information of transmission rate to the $CR(t)$ predictor. Note that, we propose to control the magnitude of $\tau'_p(t; \Theta)$ at \hat{t}_E instead of imposing the equality constraint $\tau'_p(\hat{t}_E; \Theta) = 0$, so as to reduce the impact of prediction error in the preceding logistic regression.

When λ_0 is tunable, Problem (11) is equivalent to the following formulation:

$$CR^* = \arg \min_{P(\cdot; \Theta) \in P_m} \frac{1}{N} \sum_{i=1}^N \left(CR(t_i) - P(t_i; \Theta) \right)^2 + \lambda \left(\tau'_p(\hat{t}_E; \Theta) \right)^2, \tag{12}$$

where $\lambda > 0$ is the hyperparameter. Problem (11) is a classical composition of optimization problem for learning models, with a data term and a regularization term which aims to address the ill-posedness of the original problem and/or to endow the additional characteristics of the optimizer. λ controls the influence of regularization term. The greater λ is, the smaller $\tau'_p(\hat{t}_E; \Theta^*)$ will be.

Recall the comments at the end of Section II-B, compared to forecasting $\tau(t)$ and use its deduced $CR(t)$ values as future prediction, forecasting $CR(t)$ directly as in Problem (11) with more accurate $\tau(t)$ information will avoid the error accumulation in the SIRU model, hence lead to a more satisfactory $CR(t)$ forecasting.

We now provide the explicit formula of $\tau'_p(t)$ in Problem (11). When $\widehat{CR}(t)$ is given as the polynomial $P(t; \Theta) \in P_m$, solving directly the SIRU model (9)

gives the corresponding transmission rate:

$$\tau'_p = \frac{\ddot{I} + v\dot{I}}{(I + U)S} - \frac{(\dot{I} + vI)\dot{S}}{(I + U)S^2} - \frac{(\dot{I} + vI)(\dot{I} + \dot{U})}{(I + U)^2 S},$$

where

$$\begin{aligned} I &= \frac{1}{v_1} \dot{P}, \quad \dot{I} = \frac{1}{v_1} \ddot{P}, \\ S &= -I - \frac{v}{v_1} P + c_s, \quad \dot{S} = -\dot{I} - vI, \\ U &= \frac{v_2}{\eta} \sum_{k=0}^{m-1} \frac{(-1)^k}{\eta^k} I^{(k)} + c_u \exp(-\eta t), \\ \dot{U} &= -v_2 \sum_{k=1}^{m-1} \frac{(-1)^k}{\eta^k} I^{(k)} - \eta c_u \exp(-\eta t). \end{aligned} \tag{13}$$

Thus, τ'_p can be essentially expressed in terms of $P(t; \Theta)$. Note that, to determine the constant c_s , usually we only need one function value $S(t_s)$. However, we would like to fully use the training data, and make the estimated model S as general as possible. Thus, we employ the least square estimation to evaluate constant c_s as:

$$\hat{c}_s := \arg \min_c \frac{1}{N} \sum_{i=1}^N \left(S(t_i) + I(t_i; \Theta) + \frac{v}{v_1} P(t_i; \Theta) - c \right)^2,$$

where $S(t_i)$, $i = 1, \dots, N$, are the solutions of System (9) evaluating at time t_i . Thus

$$\hat{c}_s = \frac{1}{N} \sum_{i=1}^N \left(S(t_i) + I(t_i; \Theta) + \frac{v}{v_1} P(t_i; \Theta) \right) \tag{14}$$

is also a function of Θ . Similarly, the least square estimation of c_u is

$$\begin{aligned} \hat{c}_u &= \frac{1}{N} \sum_{i=1}^N \left(U(t_i) \exp(\eta t_i) \right. \\ &\quad \left. - \frac{v_2}{\eta} \sum_{k=0}^{m-1} \frac{(-1)^k}{\eta^k} I^{(k)}(t_i; \Theta) \exp(\eta t_i) \right). \end{aligned} \tag{15}$$

Thus, we inject the terms in (14) and (15) into the Formula (13). In Section III, we will illustrate the performance of the proposed predictor CR^* using the official COVID-19 data from the government of Chile.

III. NUMERICAL EVIDENCE

In this numerical study, we consider the evolution of the COVID-19 pandemic in Chile for the period from March 2020 to December 2020, due to the availability of quarantine percentage information. We obtain the

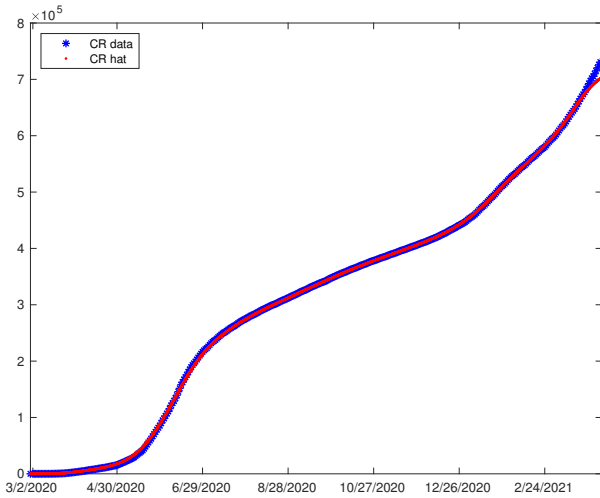


Fig. 3: Nonlinear approximation of $CR(t)$ data. The kernel smoother used here writes as: $\widehat{CR}(t) = \frac{\sum_i z_i(t) CR(t_i)}{\sum_i z_i(t)}$, where $z_i(t) = \exp(-\frac{(t-t_i)^2}{128})$.

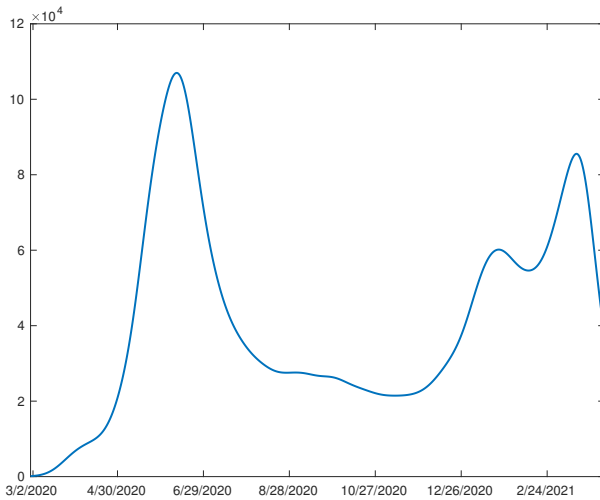


Fig. 4: Estimation of $I(t)$ based on Equation (7) from the estimation of $CR(t)$ in Figure 3.

$CR(t)$ data from the daily reported new infected cases as its cumulative sum, and the quarantine percentage from [25]. We fix $f = 0.3$, $v = 1/7$, $n = 1/7$, and $S_0 = 19458310$ (total population of Chile) throughout the experiments. We use the first 20 CR observations to fit the exponential growing and calculate the initial data. The initial data supplementing System (9) are: $t_0 = -0.6951$, $I_0 = 7.1934$, and $U_0 = 1.5945$. We first show the estimation results from the methods proposed in Section II-A. The $CR(t)$ data and its approximation by kernel smoother $\widehat{CR}(t)$ is given in Figure 3, with

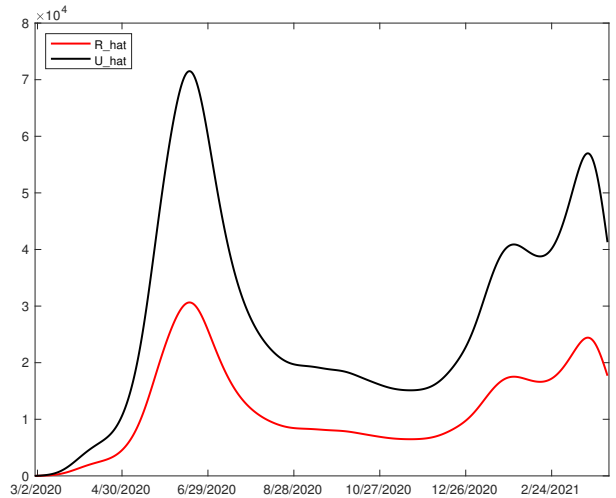


Fig. 5: Estimation of $R(t)$ and $U(t)$ based on System (9).

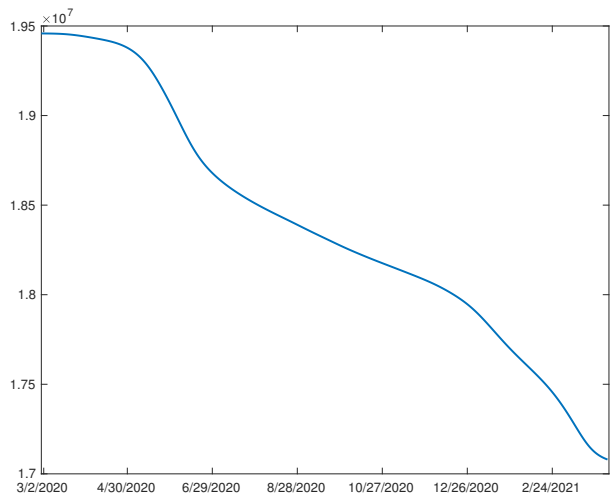


Fig. 6: Estimation of $S(t)$ based on System (9).

the corresponding $\hat{I}(t)$ given in Figure 4.

The estimations of $R(t)$, $U(t)$ and $S(t)$ as the solution of System (9) are given in Figures 5 and 6. Using these estimations, the inferred transmission rate has been shown in Figure 2, which has a consistent interpretation with respect to the quarantine percentage data.

Next, we show the result of Logistic regression. We use the inferred $\tau(t)$ data and the quarantine percentage data until 9/02/2020 to train the logistic model (10). Then the fitted model is used to forecast the probability of occurrence of $\hat{\tau} = 0$ from September to December with the corresponding quarantine percentage data. We compare the prediction result in Figure 7 with the “true” $\tau(t)$ data, where the blue curve is the predicted proba-

bility. We can see that for the training data, the model has successfully predicted its local extreme points such as the one in the beginning of May 2020, and the one at the end of June 2020. For the test data, the model forecasts that around 11/01/2020 and 12/18/2020, there will likely appear local extreme points of $\tau(t)$, while it predicts in October, it will be almost impossible to appear extreme points.

We now use these predicted moments \hat{t}_E to derive the predictor of $CR(t)$ as proposed in Equation (12), and compare their values with the true data values. To evaluate the performance of predictor, especially to examine the improvement brought by the information of future τ which is well predicted from quarantine percentage, we set the fitting interval t_1, \dots, t_N at least half a month earlier than the predicted local extreme point of $\tau(t)$, and fit it with a polynomial without shape control as well as a polynomial with the proposed shape control by \hat{t}_E . For $\hat{t}_E = 11/01/2020$, we set the fitting interval as $t_1 = 8/13/2020$ to $t_N = 10/12/2020$ in Equation (12). While for $\hat{t}_E = 12/08/2020$, we test two fitting intervals, one spanning from $t_1 = 9/02/2020$ to $t_N = 11/01/2020$, the other from $t_1 = 9/22/2020$ to $t_N = 11/21/2020$. The order for all polynomials are fixed as $m = 4$. We try 3 λ values for each fitting intervals: 10^{36} , 50^{36} , and 10^{37} . The numerical evidence of our methods are provided in Figure 8 and Figure 9. In both figures, the blue curves refer to the real CR data while the red curves refers to the predictions from the proposed predictor, where their thin part corresponds to the fitting interval, and their thick part refer to the forecasting of a month. The green curve is the forecasting from the polynomial without shape control, which is fitted on the same interval.

In Figure 8, the plots show the one-month forecasting of CR from the proposed method incorporating the information of the forecasted extreme point $\hat{t}_E = 12/08/2020$, with different weights λ . We can see that in general, by incorporating the τ information, the forecasted values have been improved in all three λ cases, especially when $\lambda = 10^{37}$, the proposed method gives the perfect forecasting.

In Figure 9, the plots show the one-month forecasting of CR from $\hat{t}_E = 12/08/2020$ with the other fitting and predicting intervals. We can see that in this case, the best forecasting result is given by $\lambda = 50^{36}$. We would also like to report the result in the bottom subfigure of Figure 9, where the λ value is set too large for this fitting interval. In this case, since the weight of regularization loss is greater, the optimization problem (12) needs to search the polynomials of smaller

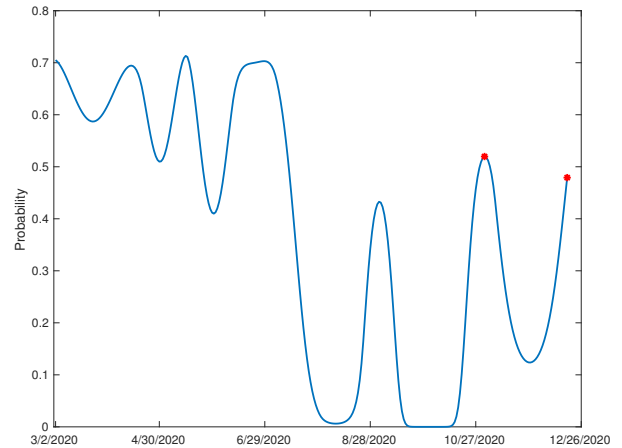


Fig. 7: The blue curve is the prediction of the probability of $\hat{\tau}(t) = 0$ based on $Q(t)$ and $\hat{Q}(t)$. The model is fitted using the data until 9/02/2020. The two red points denote the predicted future time instants \hat{t}_E , with the high predicted probabilities $P(\hat{\tau}(\hat{t}_E) = 0 | \hat{Q}(\hat{t}_E), \hat{Q}(\hat{t}_E))$. They are on the dates 11/01/2020 and 12/18/2020.

regularization loss $\tau'_p(\hat{t}_E)^2$. Such polynomials may have in return relatively larger data term loss. Thus, the optimal polynomial has a worse fitting performance.

Lastly, Figure 10 shows the forecasting performance of the CR predictor with $\hat{t}_E = 11/01/2020$. We can see that, in this case, the regularization terms have very little influence on the polynomial shapes, with all the forecasting from the proposed predictor overlapping the forecasting of the polynomial without shape control. The possible reason can be that, the polynomial without shape control has already a good prediction performance, namely, a low data term loss, meanwhile the λ values are relatively low for this fitting interval.

IV. CONCLUSION

In this paper, we firstly proposed a novel way to infer the transmission rate based on the nonparametric estimation. This proposed method has solved the problem that, with multiple epidemic waves, it is very difficult to find an accurate parametric form of transmission rate which can recover the true $CR(t)$ data. It has also considerably increased the use efficiency of the available data, instead of only using it in the hyperparameter tuning. The inferred transmission rate function enables us to furthermore establish a more sophisticated model between the epidemic and the government control. Thus, the extra government control information, which is the quarantine percentage in our case, can be used to

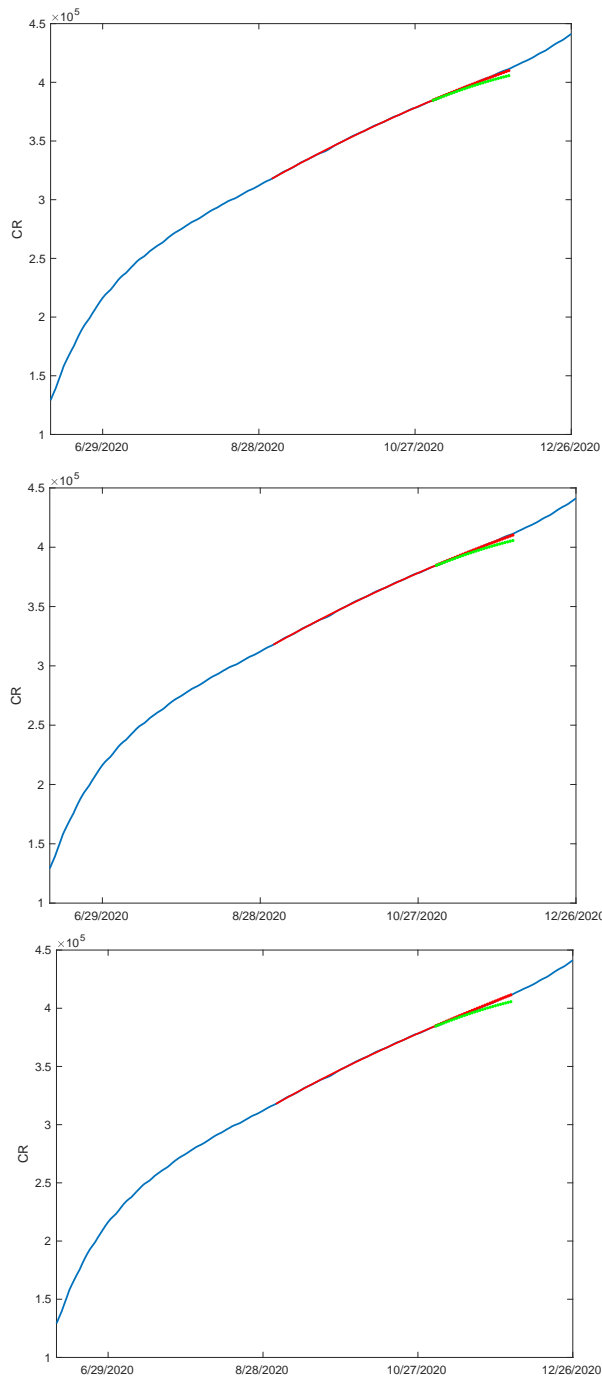


Fig. 8: CR predictor with fitting interval $t_1 = 9/02/2020$ to $t_N = 11/01/2020$, $m = 4$, $\lambda = 10^{36}$ (left), 50^{36} (right), 10^{37} (bottom), and $\hat{t}_E = 12/08/2020$.

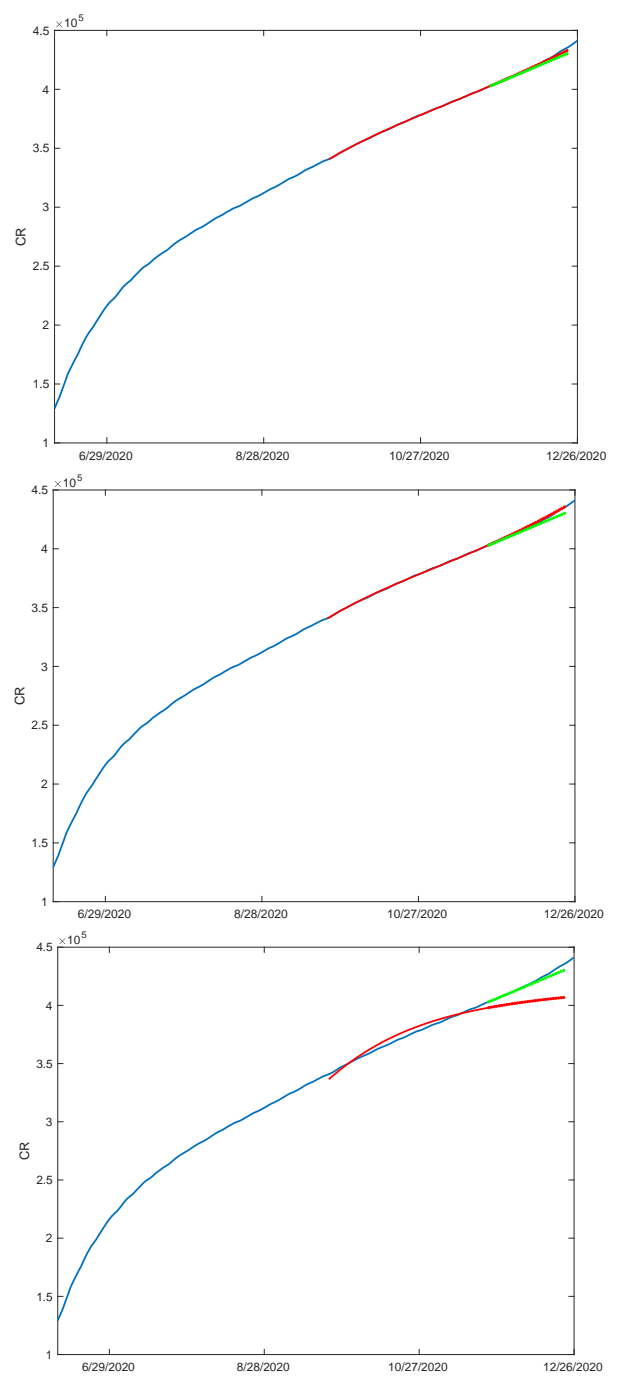


Fig. 9: CR predictor with fitting interval $t_1 = 9/22/2020$ to $t_N = 11/21/2020$, $m = 4$, $\lambda = 10^{36}$ (left), 50^{36} (right), 10^{37} (bottom), and $\hat{t}_E = 12/08/2020$.

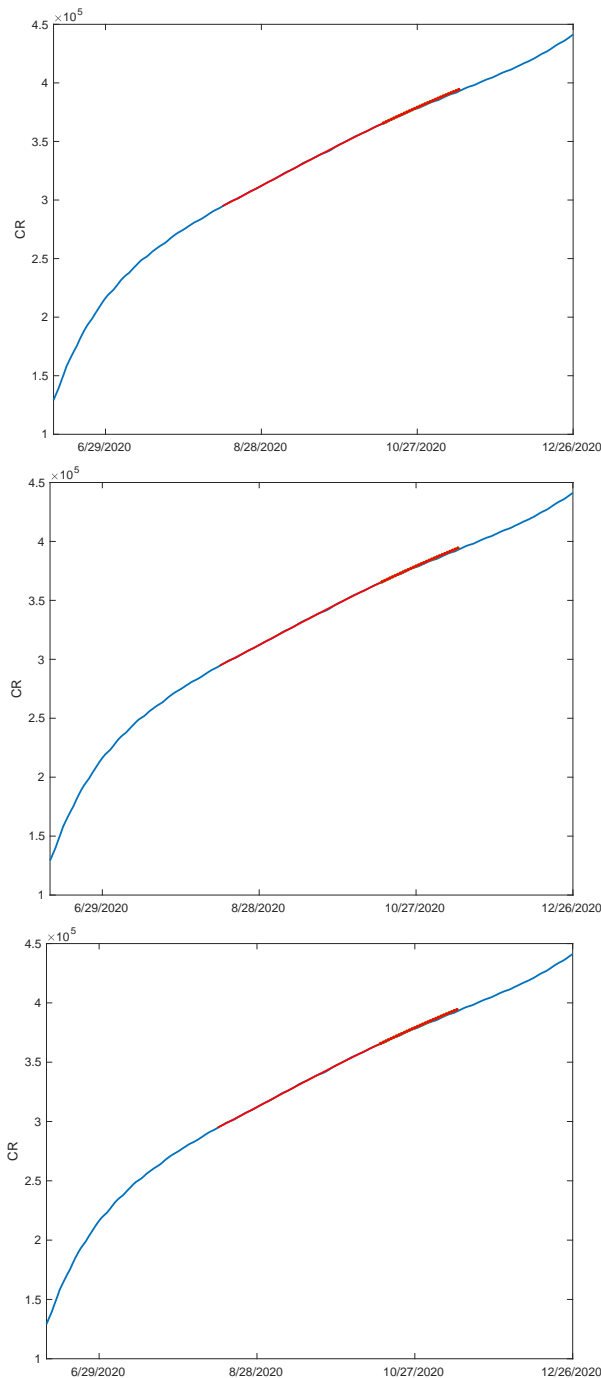


Fig. 10: CR predictor with fitting interval $t_1 = 8/13/2020$ to $t_N = 10/12/2020$, $m = 4$, $\lambda = 10^{36}$ (left), 50^{36} (right), 10^{37} (bottom), and $\hat{t}_E = 11/01/2020$.

improve the prediction of $CR(t)$. The numeric results have shown that the proposed $CR(t)$ predictor has a promising performance in terms of both accuracy and the length of efficient prediction interval, which can reach one month in our experiments.

APPENDIX

In the following we explain how to approximate a function $Q \in C^2(\mathbb{R})$ from the data points of quarantine percentage (see the right plot in Figure 2). To primarily filter out the intense fluctuations, we first subsample the data points by a frequency of 25, then we use the kernel smoother with kernel $\exp(-\frac{(t-t')^2}{18})$ on the subsampled points to generate the smooth approximation of data, denoted as \hat{Q} , which is the red curve in Figure 2. To furthermore obtain the functions of \dot{Q} and \ddot{Q} , we fit \hat{Q} with the cubic spline, and use the derivatives of the fitted spine as \dot{Q} and \ddot{Q} . Similarly, we fit the inferred transmission rate with cubic spline and use its derivative to obtain function $\hat{\tau}$.

To train Logistic model (10), we need to provide the balanced set which consists in the moments t_i^0 whose $\tau(t_i^0)$ are extremas as well as the t_j^1 whose $\tau(t_j^1)$ are not extremas. We also need the predictor quarantine percentage function values at these points, namely $\hat{Q}(t_i^0)$, $\dot{\hat{Q}}(t_i^0)$, $\ddot{\hat{Q}}(t_i^0)$, $\hat{Q}(t_j^1)$, and $\dot{\hat{Q}}(t_j^1)$. Given $\hat{\tau}$, we use the bisection method to find its roots so as to determine the moments t_i^0 . The root finding results show there are 4 extreme points before 9/02/2020, which are 4/11/2020, 5/07/2020, 6/30/2020, and 8/30/2020. We also consider their six nearest neighbouring dates as t_i^0 , to increase the training samples also to compensate any errors during the calculation. For the moments t_j^1 , we choose the dates 3/22/2020, 4/24/2020, 6/03/2020, 7/30/2020, and their six nearest neighbouring dates.

The Matlab codes implementing the numeric studies in this work are available on https://github.com/yiyej/Extended_SIRU_with_dynamic_transmission_rate.

REFERENCES

- [1] Q. Griette, J. Demongeot, P. Magal, What can we learn from COVID-19 data by using epidemic models with unidentified infectious cases?, *Mathematical Biosciences and Engineering*, 19:537–594, 2022.
- [2] Z. Liu, P. Magal, O. Seydi, G. Webb, Understanding Unreported Cases in the COVID-19 Epidemic Outbreak in Wuhan, China, and the Importance of Major Public Health Interventions, *Biology*, 9:50, 2020.
- [3] Y. Xiang, Y. Jia, L. Chen, L. Guo, B. Shu, E. Long, COVID-19 epidemic prediction and the impact of public health interventions: A review of COVID-19 epidemic models, *Infectious Disease Modelling*, 6:324–342, 2021.

- [4] C. Hou, J. Chen, Y. Zhou, L. Hua, J. Yuan, S. He, Y. Guo, S. Zhang, Q. Jia, C. Zhao, J. Zhang, G. Xu, E. Jia, The effectiveness of quarantine of Wuhan city against the Corona Virus Disease 2019 (COVID-19): A well-mixed SEIR model analysis, *Journal of Medical Virology*, 92:841–848, 2020.
- [5] Z. Yang, Z. Zeng, K. Wang, S.-S. Wong, W. Liang, M. Zanin, P. Liu, X. Cao, Z. Gao, et al., Modified SEIR and AI prediction of the epidemics trend of COVID-19 in China under public health interventions, *Journal of Thoracic Disease*, 12:165-174, 2020.
- [6] C. Anastassopoulou, L. Russo, A. Tsakris, C. Siettos, Data-based analysis, modelling and forecasting of the COVID-19 outbreak, *PLOS ONE*, 15:e0230405, 2020.
- [7] D. Fanelli, F. Piazza, Analysis and forecast of COVID-19 spreading in China, Italy and France, *Chaos, Solitons & Fractals*, 134:109761, 2020.
- [8] C. Carroll, S. Bhattacharjee, Y. Chen, P. Dubey, J. Fan, Á. Gajardo, X. Zhou, H.-G. Müller, J.-L. Wang, Time dynamics of COVID-19, *Scientific Reports*, 10:21040, 2020.
- [9] Á. Gajardo, H.-G. Müller, Point process models for COVID-19 cases and deaths, *Journal of Applied Statistics*, 50:2294–2309, 2021.
- [10] Z. Hu, Q. Ge, S. Li, L. Jin, M. Xiong, Artificial Intelligence Forecasting of COVID-19 in China, arXiv:2002.07112, 2020.
- [11] B. Nikparvar, M. Rahman, F. Hatami, J.-C. Thill, Spatio-temporal prediction of the COVID-19 pandemic in US counties: modeling with a deep LSTM neural network, *Scientific Reports*, 11:21715, 2021.
- [12] M. Shawaqfah, F. Almomani, Forecast of the outbreak of COVID-19 using artificial neural network: Case study Qatar, Spain, and Italy, *Results in Physics*, 27:104484, 2021.
- [13] R. Anguelov, J. Banasiak, C. Bright, J. Lubuma, R. Ouifki, The big unknown: The asymptomatic spread of COVID-19, *Biomath*, 9:2005103, 2020.
- [14] B. Tang, X. Wang, Q. Li, N. L. Bragazzi, S. Tang, Y. Xiao, J. Wu, Estimation of the Transmission Risk of the 2019-nCoV and Its Implication for Public Health Interventions, *Journal of Clinical Medicine*, 9:462, 2020.
- [15] Q. Griette, P. Magal, O. Seydi, Unreported Cases for Age Dependent COVID-19 Outbreak in Japan, *Biology*, 9:132, 2020.
- [16] Z. Liu, P. Magal, G. Webb, Predicting the number of reported and unreported cases for the COVID-19 epidemics in China, South Korea, Italy, France, Germany and United Kingdom, *Journal of Theoretical Biology*, 509:110501, 2021.
- [17] A. Navas, G. Vergara-Hermosilla, On the dynamics of the Coronavirus epidemic and the unreported cases: the Chilean case, arXiv:2006.02632, 2020.
- [18] T. Hastie, R. Tibshirani, J. Friedman, *The Elements of Statistical Learning: Data Mining, Inference, and Prediction*, Second Edition, Springer, New York, 2009.
- [19] S. Namasudra, S. Dhamodharavadhani, R. Rathipriya, Non-linear Neural Network Based Forecasting Model for Predicting COVID-19 Cases, *Neural Processing Letters*, 55:171–191, 2021.
- [20] O. Torrealba-Rodriguez, R. A. Conde-Gutiérrez, A. L. Hernández-Javier, Modeling and prediction of COVID-19 in Mexico applying mathematical and computational models, *Chaos, Solitons & Fractals*, 138:109946, 2020.
- [21] M. Yousaf, S. Zahir, M. Riaz, S. M. Hussain, K. Shah, Statistical analysis of forecasting COVID-19 for upcoming month in Pakistan, *Chaos, Solitons & Fractals*, 138:109926, 2020.
- [22] F. Rustam, A. A. Reshi, A. Mehmood, S. Ullah, B.-W. On, W. Aslam, COVID-19 Future Forecasting Using Supervised Machine Learning Models, *IEEE Access*, 8:101489–101499, 2020.
- [23] F. Petropoulos, S. Makridakis, Forecasting the novel coronavirus COVID-19, *PLOS ONE*, 15:e0231236, 2020.
- [24] R. J. Hyndman, G. Athanasopoulos, *Forecasting: Principles and Practice*, Second Edition, OTexts.com/fpp2, 2018.
- [25] Official data about COVID-19 from the Chilean government, in Spanish, <https://www.gob.cl/coronavirus/cifrasoficiales/>, [30-Dec-2024].